

# Total energy loss assessment for trickle lateral lines equipped with integrated in-line and on-line emitters

Gürol Yildirim

Received: 15 November 2008 / Accepted: 5 October 2009 / Published online: 20 October 2009  
© Springer-Verlag 2009

**Abstract** The accurate evaluation for the pressure head distribution along a trickle (drip) irrigation lateral, which can be operated under low-pressure head, dictates to precisely determine the total energy (head) losses that incorporate the combined friction losses due to pipe and emitters and, the additional local losses, sometimes called minor losses, due to the protrusion of emitter barbs into the flow. In routine design applications, assessment of total energy losses is usually carried out by assuming the hypothesis that minor losses can be neglected, even if the previous experimental studies indicated that minor losses can become a significant percentage of total energy losses as a consequence of the high number of emitters (with reducing the emitter spacing) installed along the lateral line. In this study, first, simple mathematical expressions for computing three energy loss components—minor friction losses through the path of an integrated in-line emitter, the local pressure losses due to emitter connections, and the major friction losses along the pipe—are deduced based on the backward stepwise procedure, which are quickly implemented in a simple Excel spreadsheet, to rapidly evaluate the relative contribution of each energy loss component to the amount of total energy losses. An approximate

combination formulation is finally proposed to evaluate total energy drop at the end of the lateral line. For practical purpose, two design figures were also prepared to demonstrate the variation of total friction losses (due to pipe and emitters) with emitter local losses, and the variation of pipe friction losses with emitter minor friction losses, versus different emitter spacing ranging from 0.2 to 1.5 m, and various total number of emitters, regarding two kinds of the integrated in-line emitters. Comprehensive comparison test covering two design applications for different kinds of integrated in-line and on-line emitters indicated that the present mathematical model is simple, can be easily adaptable, but sufficiently accurate in all design cases examined, in comparison with the alternative procedures available in the literature.

## List of symbols

$c$	Coefficient in Eq. 4
$D_i$	Lateral pipe inner diameter (mm, m)
$D_g$	Inner diameter of an integrated in-line/on-line emitter (mm, m)
$f$	The Blasius friction factor for the range of Reynolds number, $2,000 < R < 36,000$
$f_e$	Friction coefficient for the emitter flow
$g$	Acceleration due to gravity ( $\text{m s}^{-2}$ )
$h_{f(e)}$	Friction loss through individual in-line emitter (m)
$H_{av}$	Average pressure head (m)
$H_{in}, H_1$	Operating inlet pressure head or pressure head at the first upstream emitter (m)
$H_{(N)}$	Pressure head at the first emitter from the downstream closed end (m)
$I$	Integer, counted from 1 to $N$

Communicated by P. Waller.

G. Yildirim (✉)  
Faculty of Engineering, Hydraulics Division, Civil Engineering  
Department, Aksaray University, 68100 Aksaray, Turkey  
e-mail: yildirim3@itu.edu.tr

*Present Address:*  
G. Yildirim  
Biological and Agricultural Engineering Department (BAEN),  
Texas A&M University (TAMU), College Station, TX, USA

$j_e$	Emitter friction loss per unit emitter length (m/m)
$K$	Constant given by Eq. 8
$L_g$	Longitudinal length of integrated in-line emitter (mm, m)
$L_e$	Length of the lateral line between the first and last emitters (m)
$N$	Total number of emitters along the lateral
ND	Nominal diameter of the lateral pipe (mm, m)
$Q_n$	Nominal flow rate ( $L h^{-1}$ or $m^3 s^{-1}$ )
$Q_{av}$	Average flow rate ( $L h^{-1}$ or $m^3 s^{-1}$ )
$Q_{in}$	Total flow rate accumulated by all emitter outflows ( $L s^{-1}$ )
$q_n$	Emitter outflow at the downstream closed end ( $L h^{-1}$ or $m^3 s^{-1}$ )
$q_i$	Individual emitter outflow ( $L h^{-1}$ or $m^3 s^{-1}$ )
$Q$	Total lateral inflow rate ( $L h^{-1}$ or $m^3 s^{-1}$ )
$R$	Reynolds number
$R_g$	Reynolds number for the flow occurred in the integrated in-line emitter
$S$	Emitter spacing (m)
UC	Christiansen uniformity coefficient (%)
$V_g$	Flow velocity inside the emitter ( $m s^{-1}$ )
$V$	Flow velocity in the pipe ( $m s^{-1}$ )
$\Delta H_T$	Total energy (head) losses at the end of the lateral line (m)
$\Delta H_f$	Total friction losses due to pipe and emitters (m)
$\Delta H_l$	Summation of local losses due to emitter connections (m)
$\Delta H_{f(e)}$	Summation of friction losses through the paths of integrated in-line emitters (m)
$\Delta H_{f(p)}$	Total friction losses along the lateral line (m)
$\Phi_{e(l,f)}$	The ratio of total emitter local losses to the total emitter friction losses (m)
$\Phi_l$	The amount of total emitter local losses as percentage of total energy losses (m)
$\Phi_f$	The ratio of total friction losses to the total emitter local losses (m)
$\nu$	Kinematic viscosity of water at standard temperature, $\nu = 1.01 \times 10^{-6}$ ( $m^2 s^{-1}$ )
$\lambda$	Local pressure loss caused by the presence of emitter (m)
$\alpha$	Local loss coefficient

## Introduction

In a trickle irrigation system, water is distributed through small dissipating devices called emitters installed on

polyethylene pipes called laterals. Lateral pipeline is a hydraulic structure whose design is limited by the inlet pressure head and water application uniformity that is affected by the total energy losses, the field topography as well as the emitter hydraulic characteristics (Yildirim 2007b). The insertion of emitters along a trickle lateral modifies the flow streamlines, inducing local turbulence that results in additional local pressure losses, sometimes called minor losses, rather than the pipe friction losses. To accurately evaluate total energy losses in the laterals, these minor losses due to the protrusion of emitter connections in the pipe wall that must be added to the friction losses occurring in the pipe (Jeppson 1982).

On-line emitters cause the contraction and subsequent enlargement of flow streamlines due to the protrusion of emitter bars into the flow. The introduction of integrated in-line emitters determines the contraction of the flow paths at the upstream connection between the emitters and the lateral pipe, and the expansion of the flow paths immediately downstream from the emitters; because the emitters usually have a smaller diameter than the pipe, an additional minor friction losses must be considered (Provenzano and Pumo 2004).

Figure 1 presents the lateral–emitter configuration to demonstrate flow variation (upstream sudden contraction and subsequent downstream enlargement) due to the presence of (a) integrated in-line and (b) on-line emitters, and the related hydraulic characteristics along the lateral section.

In the past, numerous researches have been done on the hydraulic analysis of trickle irrigation pipeline networks. As a matter of fact, a significant amount of these researches (Wu and Gitlin 1975; Wu 1992; Wu and Yue 1993; Anyoji and Wu 1987; Scaloppi and Allen 1993; Hathoot et al. 1993; Valiantzas 1998, 2002; Vallesquino and Luque-Escamilla 2001; Yıldırım and Ağırallıoğlu 2003a, b, 2004a, b, 2005a, b, c; Yıldırım 2007a, 2009a, b, c, 2008a, b) do not taken into account the effect of local losses in the design procedure, although the importance of minor losses has been recently presented in the experimental analysis (Howell and Barinas 1980; Al-Amoud 1995; Bagarello et al. 1995, 1997; Juana et al. 2002b; Provenzano and Pumo 2004, 2006; Provenzano et al. 2005) and the alternative analytical and numerical approaches (Jeppson 1982; Kang and Nishiyama 1996; Hathoot et al. 2000; Vallesquino and Luque-Escamilla 2002; Wu 1997; Juana et al. 2002a; Yıldırım and Ağırallıoğlu 2004c, d, e; Yıldırım 2006a, b; Yıldırım and Ağırallıoğlu 2006).

Recently, Yıldırım (2007b) presented a simple analytical procedure for hydraulic design of trickle laterals which takes into consideration the effect of minor head losses expressing the amount of minor head losses as a fraction of

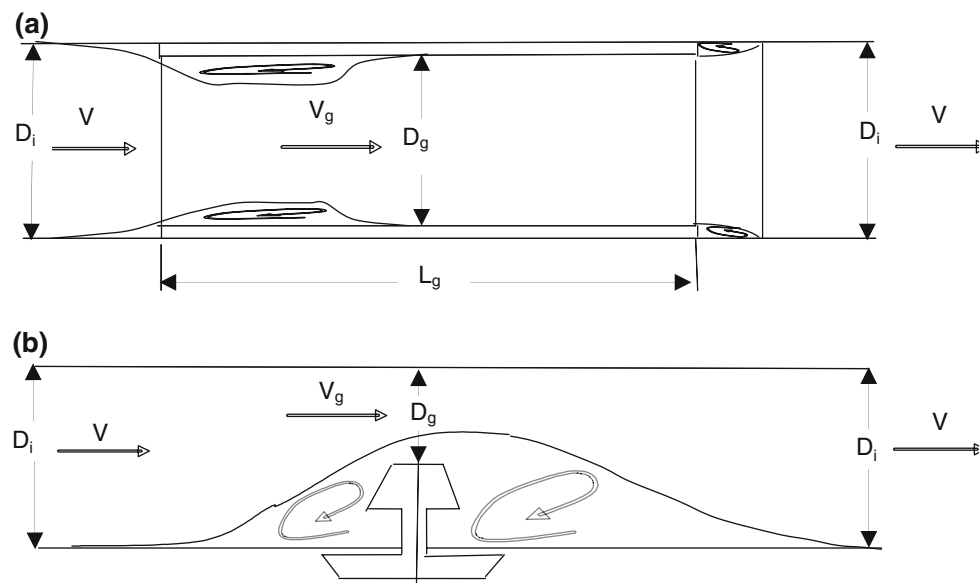


**Fig. 1** Flow variation (sudden contraction and subsequent enlargement) and hydraulic variables along lateral section with **a** integrated in-line emitter, **b** on-line emitter

the kinetic head, as well as the effect of the emitter outflow non-uniformity, the kinetic head change, the number of emitters, and different uniform line slopes on the lateral hydraulic computations. For any desired uniformity level, the analytical procedure gives one an opportunity to evaluate the influence of local energy loss on the pipe geometric characteristics (pipe size and length) and on the corresponding hydraulic variables (operating inlet and downstream end pressure heads and total energy losses). The examination results for different design combinations revealed that, in some design cases, neglecting minor losses may lead to erroneous designs of the lateral diameter and length.

This paper offers a simple mathematical model based on the stepwise procedure to accurately determine the pressure head profile along the lateral line. Essentially, the present work originally extends to the previous discussion (Yildirim 2006a, b) on the experimental analysis of local pressure losses along micro-irrigation laterals (Provenzano and Pumo 2004) to cover a systematic comparison for different kinds of in-line/on-line emitters and various design configurations. In the paper, relative contribution of each of energy loss components (emitter friction and local losses and pipe friction losses) to the amount of total energy losses is clearly evaluated using the present mathematical expressions. This procedure is also examined on the two numerical examples covering different kinds of integrated in-line and on-line emitters, and the results are compared with those of obtained from the recent analytical and experimental procedures, for all performed simulations.

### Mathematical formulation for total energy loss components

Minor friction losses through path of integrated in-line emitters

Integrated in-line emitters have an inner diameter,  $D_g$  (m), smaller than the pipe inner diameter,  $D_i$  (m), and therefore the emitters determine higher frictional head losses due to the lower cross-section area (Provenzano and Pumo 2004). For accurate evaluating total energy losses along a lateral with integrated in-line emitters, the additional friction losses occurred through the paths of in-line emitters must be taken into account. Emitter friction loss per unit emitter length,  $J_e$  (m/m), can also be evaluated by the Darcy–Weisbach formula:

$$J_e = \frac{f_e V_g^2}{D_g 2g} \quad (1)$$

where  $f_e$  = friction coefficient for the emitter flow;  $D_g$  = internal diameter of an integrated in-line emitter (m);  $V_g$  = flow velocity inside the emitter ( $\text{m s}^{-1}$ ); and  $g$  = acceleration due to gravity ( $\text{m s}^{-2}$ ).

The emitter friction loss for an individual in-line emitter,  $h_{f(e)}$ , can be evaluated from:

$$h_{f(e)} = J_e L_g \quad (2)$$

where  $L_g$  = longitudinal length of integrated in-line emitter (m).

Using the continuity equation, the following relationships between the pipe and the emitter flow velocity,  $V$  and  $V_g$ , can then be written:

$$V_g = V \left( \frac{D_i}{D_g} \right)^2 = \frac{4Q}{\pi D_g^2} \tag{3}$$

where  $V$  = flow velocity in the pipe section ( $\text{m s}^{-1}$ );  $D_i$  = lateral pipe inner diameter (m); and  $Q$  = total lateral inflow rate ( $\text{m}^3 \text{s}^{-1}$ ).

For the interval of the Reynolds number,  $R$ ,  $2,000 < R < 36,000$  for the friction coefficient,  $f$ , the Blasius equation is practically used to determine the friction losses. For a large range of the Reynolds number, for the flow into the integrated in-line emitter, the following expression can be used:

$$f_e = cR_g^{-0.25} \tag{4}$$

where  $c$  = coefficient which can be assumed to equal 0.316 (Blasius 1913) and 0.302 (Bagarello et al. 1995),  $R_g$  = Reynolds number for the flow occurred in the integrated in-line emitter which can be expressed as:

$$R_g = \frac{V_g D_g}{\nu} = \frac{4Q}{\pi \nu D_g} \tag{5}$$

where  $\nu$  = kinematic viscosity of water at standard temperature,  $\nu = 1.01 \times 10^{-6} \text{ m}^2 \text{ s}^{-1}$ .

Substituting Eq. 5 into Eq. 4, then yields:

$$f_e = c \left( \frac{\pi \nu}{4} \right)^{0.25} \left( \frac{D_g}{Q} \right)^{0.25} \tag{6}$$

Substituting Eqs. 3 and 6 into Eq. 1 and then into Eq. 2, the friction loss in the integrated in-line emitter along its length,  $L_g$ , can then be written:

$$h_{f(e)} = K \frac{Q^{1.75}}{D^{4.75}} L_g \tag{7}$$

where

$$K = c \frac{\nu^{0.25}}{2g} \left( \frac{4}{\pi} \right)^{1.75} \tag{8}$$

The value of the constant  $K$  is equal to  $7.792 \times 10^{-4}$ , if the friction coefficient is determined by using the classical Blasius formula ( $c = 0.316$ ), and  $7.447 \times 10^{-4}$ , if the value of  $c$  is taken into account 0.302 (Bagarello et al. 1995).

Assuming  $N$  emitters are located from the lateral inlet (1st emitter) toward to the downstream closed end ( $N$ th emitter), using Eq. 7, then the sum of friction losses along the integrated in-line emitters,  $\Delta H_{f(e)}$ , can be practically evaluated from the following mathematical expression:

$$\Delta H_{f(e)} = \sum_{i=1}^{i=N} \Delta H_{f(e)i} = KL_g \frac{Q_n^{1.75}}{D^{4.75}} \sum_{i=1}^{i=N} i^{1.75} \tag{9}$$

where  $Q_n$  = nominal flow rate which assumed equal to the average value of the emitter outflow ( $Q_{av}$ ) ( $\text{L h}^{-1}$ ); and

$i$  = an integer represents the consecutive order of emitters. It is assumed that the nominal value of the flow rate is approximately equal to the average flow rate when the pressure head along the lateral varies between 10% of the nominal pressure head value.

### Local energy losses due to the presence of integrated in-line/on-line emitters

The introduction of an integrated in-line or on-line emitter in a lateral causes a local pressure loss,  $\lambda$ , due to the obstruction of emitter connection into the pipe flow, that can be expressed as an “ $\alpha$ ” fraction of the kinetic head (Jeppson 1982):

$$\lambda = \alpha \frac{V^2}{2g} = \alpha \frac{8Q^2}{\pi^2 g D_i^4} \tag{10}$$

where  $\alpha$  = local loss coefficient due to both the contraction and the subsequent enlargement, can then be expressed as a function of the diameter ratio  $D_i/D_g$ , which is experimentally verified by the following expression (Provenzano and Pumo 2004; Provenzano et al. 2005):

$$\alpha = 0.056 \left[ \left( \frac{D_i}{D_g} \right)^{17.83} - 1 \right] \tag{11}$$

The amount of local pressure losses due to the presence of integrated in-line and/or on-line emitters,  $\Delta H_l$ , can be easily determined by the following mathematical expression (Provenzano et al. 2005):

$$\Delta H_l = \sum_{i=1}^{i=N-1} \Delta H_{li} = \alpha \left( \frac{8}{\pi^2 g} \right) \frac{Q_n^2}{D_i^4} \sum_{i=1}^{i=N-1} i^2 \tag{12}$$

### Major friction losses along the lateral with integrated in-line/on-line emitters

Assuming integrated in-line emitters are located at an equal spacing,  $S$ , then the sum of the friction losses along the length of the straight pipe sections between the consecutive in-line emitters,  $(S - L_g)$ , can be computed from the following expression:

$$\Delta H_{f(p)} = \sum_{i=1}^{i=N-1} \Delta H_{f(p)i} = K \frac{Q_n^{1.75}}{D_i^{4.75}} (S - L_g) \sum_{i=1}^{i=N-1} i^{1.75} \tag{13}$$

For the lateral with on-line emitters, Eq. 13 simply transforms to the following:

$$\Delta H_{f(p)} = \sum_{i=1}^{i=N-1} \Delta H_{f(p)i} = KS \frac{Q_n^{1.75}}{D_i^{4.75}} \sum_{i=1}^{i=N-1} i^{1.75} \tag{14}$$

**Total energy losses along the lateral with integrated in-line and/or on-line emitters**

As a consequence, the amount of total energy losses,  $\Delta H_T$ , is a function of three energy loss components given by Eqs. 9, 12 and 13 or 14, finally, it can be approximated by the following expression:

$$\Delta H_T = \sum_{i=1}^{i=N-1} \Delta H_{Ti} = \Delta H_{fi} + \Delta H_{li} \tag{15}$$

$$= \Delta H_{f(p)i} + \Delta H_{f(e)i} + \Delta H_{li}.$$

**Numerical applications**

For integrated in-line emitter model

In order to check the practicability of the back-step design procedure proposed in the paper, we tried to compute total head losses components using the simple formulations deduced in here. An Excel spreadsheet was carried out to set up whole hydraulic calculations.

The analysis was realized by considering two types of integrated in-line emitters B and C which are characterized by the following experimental relationships given by (Provenzano and Pumo 2004; Table 1):

B model (Siplast Tandem):  $Q_{(Lh^{-1})} = 0.612H_{(m)}^{0.537}$  (16)

C model (Rainbird Goccialin):  $Q_{(Lh^{-1})} = 0.667H_{(m)}^{0.514}$ . (17)

The analysis was realized by considering zero slope case and by setting the emitter spacing equal to the commercially existing values of 0.2, 0.4, 0.6, 0.8, 1.0, and 1.5 m. The specifications of both the emitter models are as follows:

For the B model

Nominal flow rate of the emitter outflow (as indicated by the manufacturer),  $Q_n = 2.1 \text{ L h}^{-1} = 5.833 \times 10^{-7} \text{ m}^3 \text{ s}^{-1}$ ; nominal diameter and inner diameter of the lateral pipe, ND = 16 mm and  $D_i = 13.29 \text{ mm}$ , respectively; inner diameter and longitudinal length of the integrated in-line emitter,  $D_g = 11.51 \text{ mm}$  and  $L_g = 67.89 \text{ mm}$ , respectively. The ratio of the pipe diameter to the emitter diameter,  $D_i/D_g = 1.155$ , and therefore the local loss coefficient from Eq. 11:

$$\alpha = 0.056 \left[ \left( \frac{13.29}{11.51} \right)^{17.83} - 1 \right] = 0.671.$$

For the C model

$Q_n = 2.2 \text{ L h}^{-1} = 6.111 \times 10^{-7} \text{ m}^3 \text{ s}^{-1}$ ; ND = 16 mm,  $D_i = 13.46 \text{ mm}$ ;  $D_g = 12.14 \text{ mm}$ ; and  $L_g = 68.22 \text{ mm}$ .  $D_i/D_g = 1.108$  and finally the local loss coefficient from Eq. 11,  $\alpha = 0.297$ , is computed.

Further discussion on results for this application will be presented in the following section “Results and discussion”.

For on-line emitter model

Determine the percentages of total energy (pressure) losses for two on-line emitter models (labyrinth and orifice-vortex) by considering the horizontal trickle lateral to have inner diameter,  $D = 13.4 \text{ mm}$ , and by setting the emitter spacing,  $S$ , equal to the values of 0.3, 0.6, 0.9, and 1.2 m, respectively, in terms of the overall Christiansen uniformity coefficient of the system is  $U_C = 98.8\%$ . The following relationships with local loss coefficients,  $\alpha$ , for both emitter models are experimentally verified as follows (Juana et al. 2002b):

**Table 1** Values of hydraulic characteristics for two kinds of the integrated in-line emitter models (B: *Siplast Tandem* and C: *Rainbird Goccialin*) for different emitter spacing ( $S$ ) ranging from 0.2 to 1.5 m, and various number of emitters ( $N$ ) for the desired (fixed) level of the Christiansen’s uniformity coefficient, UC = 97%, for the present mathematical model

S (m)	B model ( <i>Siplast Tandem</i> ) ( $\alpha = 0.671$ )						C model ( <i>Rainbird Goccialin</i> ) ( $\alpha = 0.297$ )					
	$N$	$L_e$ (m)	$Q_{in} = \sum_{i=1}^{i=N} q_i$ ( $\text{L h}^{-1}$ )	$H_{in} = H_{(1)}$ (m)	$H_{(N)}$ (m)	$\Delta H_T$ (m)	$N$	$L_e$ (m)	$Q_{in} = \sum_{i=1}^{i=N} q_i$ ( $\text{L h}^{-1}$ )	$H_{in} = H_{(1)}$ (m)	$H_{(N)}$ (m)	$\Delta H_T$ (m)
0.2	172	34.2	356.2	10.231	8.165	2.066	188	37.4	402.3	10.154	8.305	1.849
0.4	153	60.8	316.4	10.203	8.165	2.038	159	63.2	339.3	10.094	8.305	1.789
0.6	140	83.4	289.3	10.190	8.165	2.025	143	85.2	305.4	10.111	8.305	1.806
0.8	130	103.2	268.4	10.169	8.165	2.004	132	104.8	282.1	10.134	8.305	1.829
1.0	123	122.0	254.1	10.191	8.165	2.026	123	122.0	262.7	10.125	8.305	1.820
1.5	109	162.0	224.9	10.166	8.165	2.001	109	162.0	233.3	10.174	8.305	1.869

$N$  = total number of emitters along the lateral line;  $L_e = (N - 1) S$  = length of lateral between the first and last emitters;  $Q_{in}$  = total inflow rate which is accumulated by all emitter outflows;  $H_{in} = H_{(1)}$  = pressure head at the first emitter in lateral inlet;  $H_{(N)}$  = downstream closed end pressure head at the last emitter and;  $\Delta H_T$  = the amount of total energy (head) losses which consists of total friction and local losses

*Labyrinth on-line emitter model* [ $Q_{av} = 4.1 \text{ L h}^{-1}$ ;  $H_{av} = 9.65 \text{ m}$ ;  $\alpha = 0.34$ ]:

$$Q_{(Lh^{-1})} = 1.32H_{(m)}^{0.5}. \quad (18)$$

*Orifice-vortex on-line emitter model* [ $Q_{av} = 4.2 \text{ L h}^{-1}$ ;  $H_{av} = 10.34 \text{ m}$ ;  $\alpha = 0.67$ ]:

$$Q_{(Lh^{-1})} = 1.65H_{(m)}^{0.4}. \quad (19)$$

Detailed analysis of results and discussion on this application will be presented in the following section “[Results and discussion](#)”.

### Implementation of the stepwise procedure

The numerical stepwise procedure in the backward form based on the present mathematical model can be implemented for the data given in the present applications, starting from the downstream closed end ( $N$ th emitter) toward to the lateral inlet (1st emitter).

First, in accordance with the first application (for integrated in-line emitter model), the following calculation steps are applied, respectively:

1. The outflow of the  $N$ th emitter as a function of the corresponding pressure head was assumed to equal 90% of that corresponding to the nominal discharge. The outflows at the downstream end for the B model:  $q_N = 0.90 \times 2.1 = 1.89 \text{ L h}^{-1}$  and for the C model:  $q_N = 0.90 \times 2.2 = 1.98 \text{ L h}^{-1}$ , and the corresponding pressure heads were computed from their outflow-pressure head relationships;
2. The friction loss along both the  $N$ th emitter,  $\Delta H_{f(e)(N)}$ , by Eq. 9, and the friction loss along the pipe segment between the consecutive  $N$ th and  $(N - 1)$ th emitters,  $\Delta H_{f(p)(N-1)}$ , by Eq. 13, then the local loss due to insertion of the  $(N - 1)$ th emitter,  $\Delta H_{l(N-1)}$ , by Eq. 12, were individually evaluated;
3. The pressure head for the  $(N - 1)$ th emitter, as the pressure head for the  $N$ th emitter plus the sum of total head losses between the two consecutive emitters, then and the corresponding outflow for the  $(N - 1)$ th emitter  $q_{(N-1)}$  were determined, respectively.
4. Using the continuity equation, the lateral discharge along the pipe segment between the consecutive  $N$ th and  $(N - 1)$ th emitters was computed by assuming the residual lateral flow rate at the downstream closed end from the last emitter is equal to zero,  $Q_{(N)} = q_{(N)}$  and;  $Q_{(N-1)} = Q_{(N)} + q_{(N-1)}$ . Finally, total lateral inflow rate,  $Q_{in}$ , must be equal to the sum of whole emitter outflows,  $Q_{in} = \sum_{i=1}^{i=N} q_i$ .

5. The uniformity level of the system was evaluated with the well-known Christiansen’s uniformity coefficient,  $UC = 1 - (1/NQ_n) \sum_{i=1}^{i=N} |q_i - Q_n|$ . Noting that in the UC formula, the nominal discharge is taken into consideration as the average emitter outflow. Finally, the computation steps were improved to keep to the right the fixed value of  $UC = 97\%$ . For each computation step, the uniformity coefficient UC was evaluated, and then the steps 1, 2, 3, and 4, were repeated until the desired value of  $UC = 97\%$  was finally reached.

### Results and discussion

On Application-I (for integrated in-line emitter model)

In relation to the first application (Application-I), Tables 1 and 2 synthesize the complete results for the main hydraulic characteristics regarding two kinds of integrated in-line emitter models B ( $\alpha = 0.671$ ) and C ( $\alpha = 0.297$ ) in terms of the desired (fixed) level of uniformity,  $UC = 97\%$ .

From Table 1 for both the emitter models, the values of total inflow rate,  $Q_{in}$  (4th and 10th columns), the inlet pressure head at the upstream end,  $H_{in} = H_{(1)}$  (5th and 11th columns), and the pressure head at the downstream closed end,  $H_{(N)}$  (6th and 12th columns), then the amount of the total energy losses,  $\Delta H_T$  (7th and 13th columns) are calculated, respectively, regarding with different emitter spacing,  $S$  ranging from 0.2 to 1.5 m (1st column), various total number of emitters,  $N$  (2nd and 8th columns) and total length of the lateral line,  $L_e$  (3rd and 9th columns).

Regarding with Table 1, as the emitter spacing ( $S$ ) increases and the total number of emitters ( $N$ ) decreases, the total length of the lateral line ( $L_e$ ) increases in relation to the expression  $L_e = (N - 1) S$ , for both emitter models. The total inflow rate ( $Q_{in}$ ) decreases with decreasing in the total number of emitters [i.e., reducing the total amount of emitter outflows ( $Q_{in} = q_1 + q_2 + \dots + q_N$ )]. For both emitter models and regarding different values of the emitter spacing and total number of emitters, the inlet pressure head ( $H_{in} = H_1$ ) yields similar values around 10 m, except for a little deviation.

For the sake of comparison of the total energy (head) losses ( $\Delta H_T$ ) regarding both the emitter models, for the data sets for  $S = 1.0 \text{ m}$  ( $N = 123$ ;  $L_e = 122.0 \text{ m}$ ) and for  $S = 1.5 \text{ m}$  ( $N = 109$ ;  $L_e = 162.0 \text{ m}$ ), it is observed that the values of  $\Delta H_T$  for the B model ( $\alpha = 0.671$ ) with respect to the C model ( $\alpha = 0.297$ ) increases with increasing the amount of local losses in relation to the higher local loss coefficient, as evaluated from Eq. 10. Regarding with

**Table 2** Relative contribution of three energy loss components [ $\Delta H_f$ ,  $\Delta H_{f(p)}$ ,  $\Delta H_{f(e)}$ ] to the amount of total energy losses ( $\Delta H_T$ ) with the amount of local losses as percentage of total energy losses [ $\Phi_l$ ] and the range of emitter local losses to the emitter friction losses [ $\Phi_{e(l,f)}$ ], regarding two kinds of the integrated in-line emitter models (B: *Siplast Tandem* and C: *Rainbird Goccialin*), for different emitter

spacing ( $S$ ) ranging from 0.2 to 1.5 m and various number of emitters ( $N$ ) from to 109 to 188, for the desired level of the Christiansen’s uniformity coefficient, UC = 97%, according to the present mathematical model and the recent experimental procedure (Provenzano and Pumo 2004)

$S$ (m)	$N$	$L_e$ (m)	Present mathematical model							Recent experimental analysis (Provenzano and Pumo 2004)						
			$\Delta H_T$ (m)		$\Delta H_f$ (m)		$\Phi_{e(l,f)} = \frac{\Delta H_l}{\Delta H_{f(e)}} = \frac{\Delta H_l}{\Delta H_{f(p)} + \Delta H_{f(e)}}$	$\Phi_l = \frac{\Delta H_l}{\Delta H_T}$ (%)	$\Delta H_T$ (m)		$\Delta H_f$ (m)		$\Phi_{e(l,f)} = \frac{\Delta H_l}{\Delta H_{f(e)}} = \frac{\Delta H_l}{\Delta H_{f(p)} + \Delta H_{f(e)}}$	$\Phi_{e(l,f)} = \frac{\Delta H_l}{\Delta H_{f(e)}} = \frac{\Delta H_l}{\Delta H_{f(p)} + \Delta H_{f(e)}}$ (%)		
			$\Delta H_f$	$\Delta H_l$	$\Delta H_{f(p)}$	$\Delta H_{f(e)}$			$\Delta H_f$	$\Delta H_l$	$\Delta H_{f(p)}$	$\Delta H_{f(e)}$				
<b>B model (<i>Siplast Tandem</i>) (<math>\alpha = 0.671</math>)</b>																
0.2	172	34.2	1.031	1.035	0.511	0.520	1.99	50.1	0.969	0.95	0.482	0.487	1.95	49.5		
0.4	153	60.8	1.309	0.729	0.932	0.377	1.93	35.8	1.231	0.67	0.878	0.353	1.90	35.2		
0.6	140	83.4	1.467	0.559	1.171	0.296	1.89	27.6	1.38	0.514	1.103	0.277	1.85	27.1		
0.8	130	103	1.556	0.448	1.315	0.241	1.86	22.4	1.465	0.411	1.239	0.226	1.82	21.9		
1.0	123	122	1.645	0.379	1.438	0.207	1.83	18.7	1.550	0.349	1.356	0.194	1.80	18.4		
1.5	109	162	1.737	0.265	1.588	0.149	1.78	13.2	1.636	0.243	1.496	0.140	1.74	12.9		
<b>C model (<i>Rainbird Goccialin</i>) (<math>\alpha = 0.297</math>)</b>																
0.2	188	37.4	1.226	0.623	0.664	0.562	1.11	33.7	1.156	0.573	0.626	0.530	1.08	33.1		
0.4	159	63.2	1.412	0.377	1.057	0.355	1.06	21.1	1.33	0.347	0.996	0.334	1.04	20.7		
0.6	143	85.2	1.531	0.275	1.266	0.265	1.04	15.2	1.444	0.253	1.194	0.250	1.01	14.9		
0.8	132	105	1.612	0.216	1.399	0.213	1.01	11.8	1.521	0.199	1.320	0.201	0.99	11.6		
1.0	123	122	1.644	0.175	1.469	0.175	1.0	9.6	1.551	0.161	1.385	0.166	0.97	9.4		
1.5	109	162	1.747	0.122	1.621	0.126	0.97	6.5	1.649	0.112	1.530	0.119	0.94	6.4		

$\Delta H_T$  = amount of total energy losses;  $\Delta H_f$  = amount of total friction losses due to pipe and emitters;  $\Delta H_l$  = amount of local losses due to emitter connections;  $\Delta H_{f(p)}$  and  $\Delta H_{f(e)}$  = amount of friction loss components due to pipe and emitters, respectively;  $\Phi_{e(l,f)} = \Delta H_l / \Delta H_{f(e)}$  = the ratio of total emitter local losses to total emitter friction losses;  $\Phi_l = \Delta H_l / \Delta H_T$  = the amount of emitter local losses as percentage of total energy losses (%)

different emitter spacing values, the  $\Delta H_T$  yields fixed values except for a little deviation; for the B model, the  $\Delta H_T$  values vary from 2.0 to 2.07 m, and for the C model, it yields between 1.79 and 1.87 m.

Furthermore, in order to do a systematic analysis for three components ( $\Delta H_l$ ,  $\Delta H_{f(p)}$  and  $\Delta H_{f(e)}$ ) of total energy losses ( $\Delta H_T$ ), for both the emitter models B and C, regarding with different emitter spacing,  $S$  ranging from 0.2 to 1.5 m (1st column), various total number of emitters,  $N$  (2nd column) and total length of the lateral line,  $L_e$  (3rd column), the following energy loss patterns are computed, and the results are synthesized, in Table 2. In this table first, the total energy losses ( $\Delta H_T$ ) are divided by the total friction drop ( $\Delta H_f$ ) [4th and 10th columns] and total local energy losses due to emitter connections ( $\Delta H_l$ ) [5th and 11th columns], and then the total friction losses ( $\Delta H_f$ ) are subdivided by the major friction losses along the pipe ( $\Delta H_{f(p)}$ ) [6th and 12th columns] and minor friction losses ( $\Delta H_{f(e)}$ ) [7th and 13th columns] which occurred through the paths of integrated in-line emitters, together with the ratio of emitter local losses to the emitter friction losses [ $\Phi_{e(l,f)} = \Delta H_l / \Delta H_{f(e)}$ ] [8th and 14th columns], and the emitter local losses as percentage of total energy losses

[ $\Phi_l(\%) = \Delta H_l / \Delta H_T$ ] [9th and 15th columns] are computed, respectively, from the proposed mathematical model, and the results are compared with the recent experimental analysis (Provenzano and Pumo 2004).

From this table, the analysis for three energy loss components reveals that the emitter local losses ( $\Delta H_l$ ) and the emitter minor friction losses ( $\Delta H_{f(e)}$ ) decrease due to decreasing in the total number of emitters ( $N$ ) [i.e., with increasing in the emitter spacing ( $S$ )], whereas the pipe friction losses ( $\Delta H_{f(p)}$ ) [i.e., the total friction losses ( $\Delta H_f$ )] increase due to increasing in the total length of the lateral line ( $L_e$ ). Finally, the amount of total energy losses ( $\Delta H_T$ ) (which is combination of total friction and emitter local losses) does not change more, except for a little deviation (please see, 7th and 13th columns, in Table 1), since the total increasing in the amount of  $\Delta H_f$  is just balanced with the total decreasing in the amount of  $\Delta H_l$ .

From the results obtained for the energy loss patterns [presented in the 4th, 5th, 6th, and 7th columns], the following findings can be observed. For both the emitter models B and C, first, the discrepancy between the amount of the  $\Delta H_f$  and the  $\Delta H_l$ ; and between the amount of the  $\Delta H_{f(p)}$  and the  $\Delta H_{f(e)}$  more increases as the total number of

emitters ( $N$ ) decreases and the total length of the lateral line ( $L_e$ ) increases.

However, as an exceptional case for the B emitter model, if the smallest given value of the emitter spacing ( $S = 0.2$  m) is selected ( $N = 172$  and  $L_e = 34.2$  m), there is no difference between the amount of related energy loss patterns, since the amount of emitter local losses ( $\Delta H_l = 1.035$  m) nearly identical to the amount of total friction losses ( $\Delta H_f = 1.031$  m); and the amount of emitter friction losses ( $\Delta H_{f(e)} = 0.52$  m) closely follows the amount of pipe friction losses ( $\Delta H_{f(p)} = 0.511$  m). For  $S = 0.2$  m, these results are also verified by the recent experimental work (Provenzano and Pumo 2004) as follows:  $\Delta H_f = 0.969$  m with  $\Delta H_l = 0.95$  m and  $\Delta H_{f(p)} = 0.482$  m with  $\Delta H_{f(e)} = 0.487$  m, respectively.

For the B emitter model, the ratio of emitter local losses to the emitter friction losses [8th column] generally yields around 2.0 (for  $S = 0.2$  m,  $\Phi_{e(l,f)} = 1.99$ ) and finally little decreases to 1.78 for  $S = 1.5$  m. The emitter local losses as the percentage of total energy losses [9th column] reach to the highest range of 50% [for  $S = 0.2$  m,  $\Phi_l = 50.1\%$ ] and rapidly decreases to 13.2% (for  $S = 1.5$  m). The experimental analysis gives similar results as follows:  $\Phi_{e(l,f)}$  values are 1.95 for  $S = 0.2$  m and 1.74 for  $S = 1.5$  m; and  $\Phi_l$  values are 49.5 (%) for  $S = 0.2$  m and 12.9% for  $S = 1.5$  m.

For the C emitter model, with respect to the B model (regarding with 4th–7th columns) for the smallest value of emitter spacing,  $S = 0.2$  m, the amount of total friction losses [ $\Delta H_f = 1.226$  m] is approximately equal to two times of the amount of emitter local losses [ $\Delta H_l = 0.623$  m], since the amount of emitter local losses decrease in proportion to the value of the local loss coefficient for the C model ( $\alpha = 0.297$ ) which is approximately half of the value for the B model ( $\alpha = 0.671$ ). As also previously pointed out, for the B emitter model (for  $S = 0.2$  m), the amount of emitter friction losses [ $\Delta H_{f(e)} = 0.562$  m] nearly approaches to the amount of pipe friction losses [ $\Delta H_{f(p)} = 0.664$  m], for the C emitter model, as well. For  $S = 0.2$  m, these findings are also justified with those of obtained in the recent experimental work (Provenzano and Pumo 2004) as follows:  $\Delta H_f = 1.156$  m with  $\Delta H_l = 0.573$  m and  $\Delta H_{f(p)} = 0.626$  m with  $\Delta H_{f(e)} = 0.53$  m, respectively.

For the C emitter model, the ratio of emitter local losses to the emitter friction losses [8th column] generally yields around 1.0 [for  $S = 0.2$  m,  $\Phi_{e(l,f)} = 1.11$ ] and little decreases to 0.97 for  $S = 1.5$  m. The emitter local losses as the percentage of total energy losses [9th column] approach to the range of 34% [for  $S = 0.2$  m,  $\Phi_l = 33.7\%$ ] and rapidly decrease to 6.5% for  $S = 1.5$  m. As a consequence, there is a good agreement with those of the experimental analysis as:  $\Phi_{e(l,f)}$  values are 1.08 for  $S = 0.2$  m and 0.94 for  $S = 1.5$  m; and  $\Phi_l$  values are 33.1 (%) for  $S = 0.2$  m and 6.4% for  $S = 1.5$  m.

As a remarkable result from this table, for both the emitter models (B and C) regarding the data set given for  $S = 1.0$  m ( $N = 123$ ,  $L_e = 122.0$  m) and for  $S = 1.5$  m ( $N = 109$ ,  $L_e = 162.0$  m); the amount of pipe friction losses for the C model [ $\Delta H_{f(p)} = 1.47$  and 1.62 m] is higher than those of the B model [ $\Delta H_{f(p)} = 1.44$  and 1.59 m], since the C model has a higher nominal flow rate ( $Q_n = 2.2$  L h<sup>-1</sup>) with respect to the B model ( $Q_n = 2.1$  L h<sup>-1</sup>), even if the C model has higher values of the emitter length ( $L_g$ ) and inner lateral diameter ( $D_i$ ) than those of the B model, as concluded in Eq. 13.

For both the emitter models (B and C), regarding the data set for  $S = 1.0$  m ( $N = 123$ ,  $L_e = 122.0$  m) and for  $S = 1.5$  m ( $N = 109$ ,  $L_e = 162.0$  m); the amount of emitter friction losses for the B model [ $\Delta H_{f(e)} = 0.207$  and 0.149 m] is higher than those of the C model [ $\Delta H_{f(e)} = 0.175$  and 0.126 m], since the B model has a smaller inner emitter diameter ( $D_g = 11.51$  mm) with respect to the C model ( $D_g = 12.14$  mm), even if the B model has smaller values of the emitter length ( $L_g$ ) and nominal flow rate ( $Q_n$ ) than those of the B model, as concluded in Eq. 9.

In order to demonstrate the variation of three energy loss components to each other (friction losses due to pipe and emitters, emitter local losses, and total energy losses for both the emitter models (B and C), two figures were also prepared and represented by Figs. 2 and 3, respectively. For the B model of integrated in-line emitter, Fig. 2 illustrates variation of total friction ( $\Delta H_f$ ) [premier axis of  $y$ ] and emitter local ( $\Delta H_l$ ) losses [secondary axis of  $y$ ] regarding with different values of emitter spacing ( $S$ ) varying from 0.2 to 1.5 m [premier axis of  $x$ ], and various number of emitters ( $N$ ) from 109 to 172 [secondary axis of  $x$ ], according to both the mathematical (straight bold line) and experimental (dotted line) procedures. For the C model of integrated in-line emitter, Fig. 3 illustrates variation of total friction loss components due to pipe ( $\Delta H_{f(p)}$ ) and due to emitter ( $\Delta H_{f(e)}$ ) with regarding different values of emitter spacing ( $S$ ) varying from 0.2 to 1.5 m, and various number of emitters ( $N$ ) from 109 to 188, according to both the mathematical (straight line) and experimental (dotted line) procedures. Figs. 2 and 3 also reveal that a good justification between the results of both the mathematical and experimental procedures is observed, for all performed simulations.

#### On Application-II (for on-line emitter model)

The same calculation steps for the backward stepwise procedure clarified above are repeated (from 1st to 5th) using the related formulations given for on-line emitters (Eqs. 12, 14, 15, 18, and 19) in terms of the overall desired uniformity level, UC = 98.8%.

Table 3 synthesizes the complete results for the main hydraulic variables for two kinds of on-line emitter models



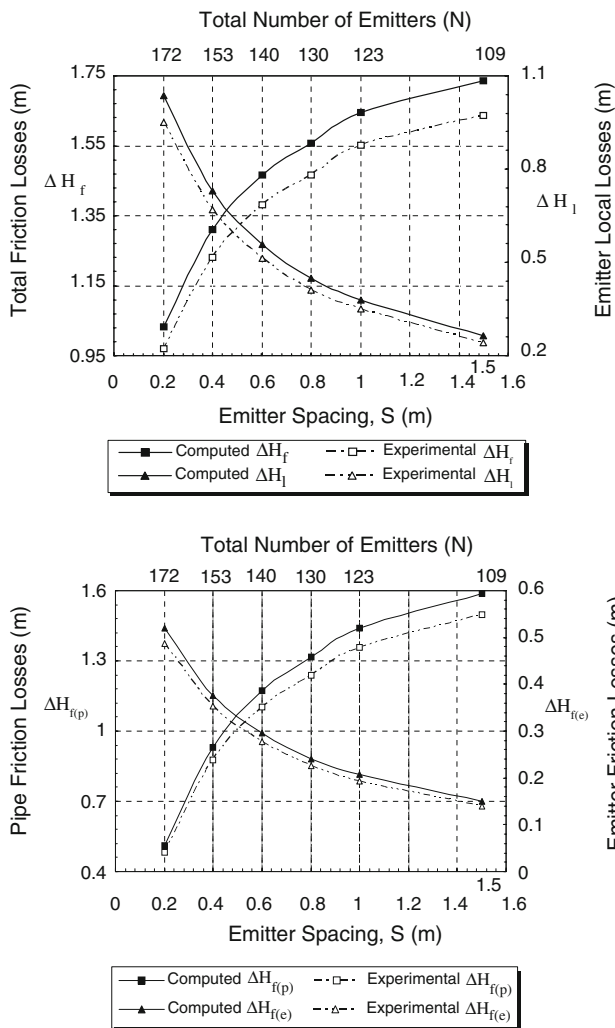


**Fig. 2** For the B model (*Siplast Tandem*) of integrated-in-line emitter, variation of total friction [ $\Delta H_f$ ] and local [ $\Delta H_l$ ] losses versus different values of emitter spacing ( $S$ ) varying from 0.2 to 1.5 m, and various number of emitters ( $N$ ), according to both the mathematical and experimental procedures

[labyrinth ( $\alpha = 0.34$ ) and orifice-vortex ( $\alpha = 0.67$ )] in comparison with those of obtained from the previous analytical procedure (Yıldırım 2007b). For the sake of comparison of the computed values for both the emitter models, two energy loss components ( $\Delta H_f$  and  $\Delta H_l$ ) [4th–8th and 5th–9th columns] to evaluate the total energy losses ( $\Delta H_T$ ), the ratio of total pipe friction losses to the emitter local losses,  $\Phi_f = \Delta H_{f(p)} / \Delta H_l$  [6th and 10th columns], and the emitter local losses as the percentage of total energy losses,  $\Phi_l = \Delta H_l / \Delta H_T$  [7th and 11th columns] regarding with different emitter spacing,  $S$  ranging from 0.3 to 1.2 m (1st column), various total number of emitters,  $N$  from 75 to 110 (2nd column), and total length of the lateral line,  $L_e$ , from 32.7 to 88.8 m (3rd column), are presented, respectively.

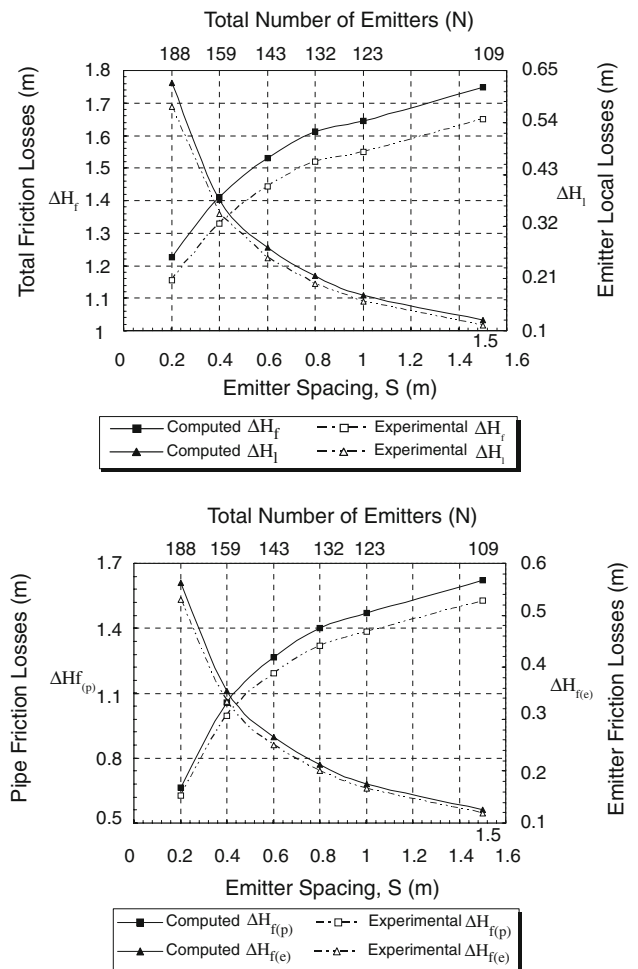


**Fig. 3** For the C model (*Rainbird Goccialin*) of integrated-in-line emitter, variation of total friction loss components due to pipe [ $\Delta H_{f(p)}$ ] and due to emitter [ $\Delta H_{f(e)}$ ] versus different values of emitter spacing ( $S$ ) varying from 0.2 to 1.5 m, and various number of emitters ( $N$ ), according to both the mathematical and experimental procedures

Regarding the values presented in this table, the following remarks can be observed. First, the values of emitter local losses for the labyrinth on-line emitter model [ $\Delta H_l = 0.598, 0.335, 0.241$  and  $0.192$  m] are approximately half of the values for the orifice-vortex on-line emitter model [ $\Delta H_l = 1.179, 0.657, 0.459$  and  $0.374$  m], since the emitter local losses proportionally increase with increasing the value of local loss coefficient,  $\alpha$  (from 0.34 to 0.67).

Practically [1st, 2nd, 3rd, 4th–8th, and 5th–9th columns], as the length of the lateral increases and the number of emitters decreases with increasing in emitter spacing, the amount of emitter local losses decreases, whereas the pipe friction losses increase; so the discrepancy between the pipe friction losses and the emitter local losses increases with increasing in the emitter spacing. For instance, regarding the smallest given value of the emitter spacing,  $S = 0.3$  m, for the labyrinth on-line emitter model

**Table 3** Relative contribution of two energy loss components [ $\Delta H_f$  and  $\Delta H_l$ ] to the amount of total energy losses [ $\Delta H_T$ ] with the range of total friction losses to the total emitter local losses [ $\Phi_f$ ], and the amount of local losses as percentage of total energy losses [ $\Phi_l$ ], regarding two kinds of the on-line emitter models (*Labyrinth and*

*orifice-vortex*), for different emitter spacing ( $S$ ) ranging from 0.3 to 1.2 m and various number of emitters ( $N$ ) from to 75 to 110, for the desired level of the Christiansen’s uniformity coefficient, UC = 98.8%, according to the present mathematical model and the previous analytical procedure (Yıldırım 2007b)

$S$ (m)	$N$	$L_e$ (m)	Present mathematical model				Previous analytical method (Yıldırım 2007b)			
			$\Delta H_T$ (m)		$\Phi_f = \Delta H_f / \Delta H_l$	$\Phi_l = \Delta H_l / \Delta H_T$ (%)	$\Delta H_T$ (m)		$\Phi_f = \Delta H_f / \Delta H_l$	$\Phi_l = \Delta H_l / \Delta H_T$ (%)
			$\Delta H_f$	$\Delta H_l$			$\Delta H_f$	$\Delta H_l$		
Labyrinth on-line emitter ( $\alpha = 0.34$ )										
0.3	110	32.70	1.215	0.598	$2.03 \cong 2.0$	32.9	1.108	0.559	$1.98 \cong 2.0$	33.5
0.6	90	53.40	1.322	0.335	$3.95 \cong 4.0$	20.2	1.277	0.307	$4.16 \cong 4.0$	19.4
0.9	80	71.10	1.421	0.241	$5.89 \cong 6.0$	14.5	1.386	0.216	$6.42 \cong 6.0$	13.5
1.2	75	88.80	1.578	0.192	$8.22 \cong 8.0$	10.9	1.548	0.178	$8.70 \cong 9.0$	10.3
Orifice-vortex on-line emitter ( $\alpha = 0.67$ )										
0.3	110	32.70	1.172	1.179	$0.99 \cong 1.0$	50.1	1.155	1.156	$0.99 \cong 1.0$	50.0
0.6	90	53.40	1.343	0.657	$2.04 \cong 2.0$	32.9	1.332	0.635	$2.10 \cong 2.0$	32.3
0.9	80	71.10	1.462	0.459	$3.18 \cong 3.0$	23.9	1.446	0.447	$3.23 \cong 3.0$	23.6
1.2	75	88.80	1.625	0.374	$4.34 \cong 4.0$	18.9	1.614	0.368	$4.38 \cong 4.0$	18.6

$\Phi_f = \Delta H_f / \Delta H_l$ : The ratio of total friction losses to the total emitter local losses;  $\Phi_l = \Delta H_l / \Delta H_T$ : the amount of total emitter local losses as percentage of total energy losses

( $\alpha = 0.34$ ), the amount of pipe friction losses is approximately equal to two times of the amount of emitter local losses, whereas for the orifice-vortex on-line emitter model ( $\alpha = 0.67$ ), the amount of pipe friction losses is approximately equal to the amount of emitter local losses.

Accordingly, for the labyrinth on-line emitter, the values of the ratio of the friction losses to the emitter local losses ( $\Phi_f$ ) are about 2, 4, 6, and 8, whereas its values are 1, 2, 3, and 4 for the orifice-vortex on-line emitter, for  $S = 0.3, 0.6, 0.9,$  and  $1.2$  m, respectively. Moreover, the amount of emitter local losses,  $\Phi_l$  (%) expressed as a percentage of the total energy losses, decreases with increasing emitter spacing, then its values can reach 32.9 and 50.1% (33.5 and 50% according to the previous analytical procedure) with respect to the labyrinth and orifice-vortex on-line emitters, respectively. It can be concluded from the complete results in this table, a good justification is observed between the results obtained from the present mathematical and the previous analytical procedures.

**Summary and conclusion**

In this paper, a simplified mathematical model based on the backward stepwise procedure which incorporates simple theoretical expressions for three energy loss components (local and friction losses due to emitters and pipe friction losses) to finally evaluate total energy losses along a trickle lateral line with integrated in-line and/or on-line emitters is presented. The proposed Eqs. 9, 13, or 14 allow one to evaluate the minor friction losses through the path of an

integrated in-line emitter and the major friction losses along the pipe, respectively; then, Eq. 12 allows one to evaluate the local losses attributable to the emitters’ connection. Finally, an approximate formulation (Eq. 15) which incorporates three energy loss components allows one to accurately evaluate total energy losses at the end of the lateral line. The present technique is applied on two numerical applications covering different types of integrated in-line and on-line emitters to demonstrate its practicability and validity with respect to the recent literature. Examination of results for applications confirmed that the proposed technique is efficient in all design cases examined and justifies with the results reported in the recent analytical and experimental procedures.

Based on the present assessment regarding different kinds of integrated in-line and on-line emitters, the following remarks can be underlined:

1. First, the amount of emitter local losses ( $\Delta H_l$ ) increases with increasing in the local loss coefficient,  $\alpha$ .
2. Reducing the length of the lateral ( $L_e$ ) and increasing the number of emitters ( $N$ ) with decreasing the emitter spacing ( $S$ ), the amount of local ( $\Delta H_l$ ) (and friction,  $\Delta H_{f(e)}$ ) losses due to the presence of emitters increases, whereas the pipe friction losses ( $\Delta H_{f(p)}$ ) (i.e., total friction losses,  $\Delta H_f$ ) decrease. For both the integrated in-line emitter models B and C (Table 2), the discrepancy between the amount of the  $\Delta H_f$  and the  $\Delta H_l$ ; and between the amount of the  $\Delta H_{f(p)}$  and the  $\Delta H_{f(e)}$  more increases as the total number of emitters ( $N$ ) decreases and the total length of the lateral line ( $L_e$ ) increases. Therefore, the amount of total energy losses ( $\Delta H_T$ ) (which is combination of total friction and emitter

local losses) does not change more, except for a little deviation (Table 1), since the total increasing in the amount of total friction losses ( $\Delta H_f$ ) is just balanced with the total decreasing in the amount of emitter local losses ( $\Delta H_l$ ).

3. For both the B and C integrated in-line emitter models (Table 1), and regarding different values of the emitter spacing ranging from 0.2 to 1.5 m, and for various total number of emitters (from 109 to 188), the inlet pressure head ( $H_{in} = H_1$ ) yields similar values around 10 m, since the amount of total energy losses ( $\Delta H_T$ ) yields fixed values, in all design cases examined.

4. The amount of emitter local losses,  $\Phi_l$ , expressed as the percentage of total energy losses ( $\Delta H_T$ ) increases with decreasing in the emitter spacing. As an exceptional case for the smallest value,  $S = 0.2$  m, the summation of emitter local losses nearly approaches to half of the amount of the total energy losses [ $\Phi_l = \Delta H_l / \Delta H_T \cong 50\%$ ].

5. For both the integrated in-line [B-siplast tandem:  $\alpha = 0.671$ ] and on-line [orifice-vortex:  $\alpha = 0.67$ ] emitters (Tables 2 and 3), and regarding the data set for the smallest value of the emitter spacing ( $S = 0.2$  or  $0.3$  m), the summation of emitter local losses nearly identical to the amount of total friction losses (due to pipe and emitters) [ $\Delta H_f \cong \Delta H_l$ ].

6. For both the B and C integrated in-line emitter models (Table 2), and regarding the data set for the smallest value of the emitter spacing ( $S = 0.2$  m), the summation of minor friction losses due to in-line emitters nearly identical to the amount of major friction losses along the pipe sections between successive in-line emitters [ $\Delta H_{f(e)} \cong \Delta H_{f(p)}$ ].

7. Regarding the data set given for different emitter spacing (from 0.2 to 1.5 m) (Table 2), if the B model ( $\alpha = 0.671$ ) is selected, the summation of emitter local losses is approximately equal to two times of the amount of emitter minor friction losses [ $\Delta H_l \cong 2 \times \Delta H_{f(e)}$ ], whereas for the C model ( $\alpha = 0.297$ ), the summation of emitter local losses is nearly identical to the summation of minor friction losses due to in-line emitters [ $\Delta H_l = \Delta H_{f(e)}$ ].

**Acknowledgments** The author would like to express his appreciation to Editor, Associate Editor and four anonymous Reviewers whose clear comments and constructive criticisms contributed greatly to the quality of the present work. Specifically, Associate Editor Dr. Peter Waller from Arizona State University is gratefully appreciated for his high contribution on its language edition. The Scientific and Technological Research Council of Turkey (TUBITAK) is also acknowledged for supporting the researcher's time at Texas A&M University by the fellowship and grants program (2219).

## References

- Al-Amoud AI (1995) Significance of energy losses due to emitter connections in trickle irrigation lines. *J Agric Eng Res* 60(1):1–5
- Anyoji H, Wu IP (1987) Statistical approach for drip lateral design. *Trans ASAE* 30(1):187–192
- Bagarello V, Ferro V, Provenzano G, Pumo D (1995) Experimental study on flow resistance law for small diameter plastic pipes. *J Irrig Drain Eng ASCE* 121(5):313–316
- Bagarello V, Ferro V, Provenzano G, Pumo D (1997) Evaluating pressure losses in drip irrigation lines. *J Irrig Drain Eng ASCE* 123(1):1–7
- Blasius H (1913) Das Aehnlichkeitsgesetz bei Reibungsvorgängen in Flüssigkeiten, Forschungsarbeiten auf dem Gebiete des Ingenieurwesens, 131(1), Germany (in German)
- Hathoot HM, Al-Amoud AI, Mohammad FS (1993) Analysis and design of trickle irrigation laterals. *J Irrig Drain Eng ASCE* 119(5):756–767
- Hathoot HM, Al-Amoud AI, Al-Mesned AS (2000) Design of trickle irrigation laterals considering emitter losses. *Int Comm Irrig Drain (ICID) J* 49(2):1–14
- Howell TA, Barinas FA (1980) Pressure losses across trickle irrigation fittings and emitters. *Trans ASAE* 23(4):928–933
- Jeppson RW (1982) Analysis of flow in pipe networks, 5th edn. Ann Arbor Science. Ann Arbor, Mich
- Juana L, Rodriguez-Sinobas L, Losada A (2002a) Determining minor head losses in drip irrigation laterals. I: methodology. *J Irrig Drain Eng ASCE* 128(6):376–384
- Juana L, Rodriguez-Sinobas L, Losada A (2002b) Determining minor head losses in drip irrigation laterals. II: experimental study and validation. *J Irrig Drain Eng ASCE* 128(6):385–396
- Kang Y, Nishiyama S (1996) Analysis and design of microirrigation laterals. *J Irrig Drain Eng ASCE* 122(2):75–82
- Provenzano G, Pumo D (2004) Experimental analysis of local pressure losses for microirrigation laterals. *J Irrig Drain Eng ASCE* 130(4):318–324
- Provenzano G, Pumo D (2006) Experimental analysis of local pressure losses for microirrigation laterals. *J Irrig Drain Eng ASCE* 132(2):193–194
- Provenzano G, Pumo D, Di Dio P (2005) Simplified procedure to evaluate head losses in drip irrigation laterals. *J Irrig Drain Eng ASCE* 131(6):525–532
- Scaloppi EJ, Allen RG (1993) Hydraulics of irrigation laterals: comparative analysis. *J Irrig Drain Eng ASCE* 119(1):91–115
- Valiantzas JD (1998) Analytical approach for direct drip lateral hydraulic calculation. *J Irrig Drain Eng ASCE* 124(6):300–305
- Valiantzas JD (2002) Continuous outflow variation along irrigation laterals: effect of the number of outlets. *J Irrig Drain Eng ASCE* 128(1):34–42
- Vallesquino P, Luque-Escamilla PL (2001) New algorithm for hydraulic calculation in irrigation laterals. *J Irrig Drain Eng ASCE* 127(4):254–260
- Vallesquino P, Luque-Escamilla PL (2002) Equivalent friction factor method for hydraulic calculation in irrigation laterals. *J Irrig Drain Eng ASCE* 128(5):278–286
- Wu IP (1992) Energy gradient line approach for direct hydraulic calculation in drip irrigation design. *Irrig Sci* 13:21–29
- Wu IP (1997) An assessment of hydraulic design of microirrigation systems. *Agric Water Manag* 32:275–284
- Wu IP, Gitlin HM (1975) Energy gradient line for drip irrigation laterals. *J Irrig Drain Eng ASCE* 101(4):323–326
- Wu IP, Yue R (1993) Drip lateral design using energy gradient line approach. *Trans ASAE* 36(2):389–394
- Yildirim G (2006a) Hydraulic analysis and direct design of multiple outlets pipelines laid on flat and sloping lands. *J Irrig Drain Eng ASCE* 132(6):537–552
- Yildirim G (2006b) Discussion of “Experimental analysis of local pressure losses for microirrigation laterals”. *J Irrig Drain Eng ASCE* 132(2):189–192
- Yildirim G (2007a) Analytical relationships for designing multiple outlets pipelines. *J Irrig Drain Eng ASCE* 133(2):140–154

- Yıldırım G (2007b) An assessment of hydraulic design of trickle laterals considering effect of minor losses. *Irrig Drain (ICID Journal)* 56(4):399–421
- Yıldırım G (2008a) Determining operating inlet pressure head incorporating uniformity parameters for multioutlet plastic pipelines”. *J Irrig Drain Eng ASCE* 134(3):341–348
- Yıldırım G (2008b) Discussion of “Turbulent flow friction factor calculation using a mathematically exact alternative to the Colebrook–White equation”. *J Hydraulic Eng ASCE* 134(8): 1185–1186
- Yıldırım G (2009a) Simplified procedure for hydraulic design of small-diameter plastic pipes. *Irrig Drain (ICID Journal)* 58(3): 209–233
- Yıldırım G (2009b) Discussion of “Field-scale assessment of uncertainties in drip irrigation lateral parameters”. *J Irrig Drain Eng ASCE* 135(2):261–263
- Yıldırım G (2009c) Discussion of “Simplified method for sizing laterals with two or more diameters”. *J Irrig Drain Eng ASCE* (accepted for publication)
- Yıldırım G, Ağralıoğlu N (2003a) Discussion of “New algorithm for hydraulic calculation in irrigation laterals”. *J Irrig Drain Eng ASCE* 129(2):142–143
- Yıldırım G, Ağralıoğlu N (2003b) Discussion of “Continuous outflow variation along irrigation laterals: effect of the number of outlets”. *J Irrig Drain Eng ASCE* 129(5):382–386
- Yıldırım G, Ağralıoğlu N (2004a) Comparative analysis of hydraulic calculation methods in design of microirrigation laterals. *J Irrig Drain Eng ASCE* 130(3):201–217
- Yıldırım G, Ağralıoğlu N (2004b) Linear solution for hydraulic analysis of tapered microirrigation laterals. *J Irrig Drain Eng ASCE* 130(1):78–87
- Yıldırım G, Ağralıoğlu N (2004c) Discussion of “Determining minor losses in drip irrigation laterals. I: methodology”. *J Irrig Drain Eng ASCE* 130(3):248–252
- Yıldırım G, Ağralıoğlu N (2004d) Discussion of “Determining minor losses in drip irrigation laterals. II: experimental study and validation”. *J Irrig Drain Eng ASCE* 130(4):344–346
- Yıldırım G, Ağralıoğlu N (2004e) Discussion of “Equivalent friction factor method for hydraulic calculation in irrigation laterals”. *J Irrig Drain Eng ASCE* 130(4):335–339
- Yıldırım G, Ağralıoğlu N (2005a) Discussion of “Inlet pressure, energy cost, and economic design of tapered irrigation sub-mains”. *J Irrig Drain Eng ASCE* 131(2):220–224
- Yıldırım G, Ağralıoğlu N (2005b) Discussion of “Explicit hydraulic design of microirrigation submain units with tapered manifold and laterals”. *J Irrig Drain Eng ASCE* 131(3):299–300
- Yıldırım G, Ağralıoğlu N (2005c) Closure to “Linear solution for hydraulic analysis of tapered microirrigation laterals”. *J Irrig Drain Eng ASCE* 131(5):490–491
- Yıldırım G, Ağralıoğlu N (2006) Closure to “Comparative analysis of hydraulic calculation methods in design of microirrigation laterals”. *J Irrig Drain Eng ASCE* 132(1):85–90